Old Dominion University
ODU Digital Commons

CCPO Publications   Center for Coastal Physical Oceanography

A Temporal Approximate Deconvolution Model for Large-Eddy Simulation

C. D. Pruett

B. C. Thomas

C. E. Grosch
Old Dominion University, cxgrosch@odu.edu

T. B. Gatski

Follow this and additional works at: https://digitalcommons.odu.edu/ccpo_pubs

Part of the Oceanography Commons, Other Oceanography and Atmospheric Sciences and Meteorology Commons, and the Physics Commons

A temporal approximate deconvolution model for large-eddy simulation

C. D. Pruett[a] and B. C. Thomas
Department of Mathematics & Statistics, James Madison University, Harrisonburg, Virginia 22807

C. E. Grosch
Departments of Ocean, Earth & Atmospheric Sciences and Computer Science, Old Dominion University, Norfolk, Virginia 23529

T. B. Gatski
Computational AeroSciences Branch, NASA Langley Research Center, Hampton, Virginia 23681

A temporal approximate deconvolution model (TADM) is developed for large-eddy simulation and is demonstrated for plane-channel flow at $Re_\tau = 590$. The TADM combines explicit causal time-domain filtering with linear deconvolution (defiltering) to approximate unfiltered fields and residual stress to arbitrarily high order. The TADM methodology appears to lead to a robust family of residual-stress models that should provide a viable alternative to conventional (spatial) filtering for applications in which spatial filtering is problematic, e.g., for problems requiring unstructured or highly stretched grids. © *2006 American Institute of Physics.* [DOI: 10.1063/1.2173288]

In 1999, Stolz and Adams[1] proposed an approximate deconvolution model (ADM) for large-eddy simulation (LES) that has performed well for flows as diverse as incompressible channel flow[2] and supersonic compression-ramp flow.[3] In the ADM, the residual stress is approximated to arbitrarily high order by deconvolving (defiltering) the resolved-scale velocity fields $\bar{u}_j$. Specifically, in the second variant of the ADM (Eq. 9 of Stolz *et al.*[2]), the exact residual stress, $R_{ij} \equiv \overline{u_i u_j} - \bar{u}_i \bar{u}_j$, is modeled as

$$M_{ij} = \overline{v_i v_j} - \bar{v}_i \bar{v}_j, \tag{1}$$

$$v_j = \sum_{k=0}^{p} C_k \bar{u}_j^{(k+1)}, \tag{2}$$

with $\bar{u}_j^{(1)} \equiv \bar{u}_j$. The deconvolved velocity v_j approximates the unfiltered velocity u_j by a linear combination of (k-time) multiply filtered fields $\bar{u}_j^{(k)}$. Here, the index p defines the *degree* of the deconvolution.

The coefficients C_k are derived indirectly from the transfer function $H(\xi)$ of the primary filter, where $\xi = \kappa\Delta$, κ is the wave number, and Δ is the spatial filter width. Provided the filter is invertible ($H \neq 0$) and $|1-H| < 1$, the transfer function has an exact power-series inverse, namely $H^{-1} = 1/[1 - (1-H)] = \sum_{k=0}^{\infty} (1-H)^k$. The exact inverse, however, is undesirable for applications to LES, for only the resolved scales are of interest. Truncating the series at finite p yields the transfer function of the approximate inverse $\tilde{H}^{-1}$, namely

$$\tilde{H}^{-1} = \sum_{k=0}^{p} (1-H)^p. \tag{3}$$

By isometry between Fourier space [Eq. (3)] and physical space [Eq. (2)], the coefficients C_k are determined simply from the binomial theorem (i.e., from Pascal's triangle).

As a generalized scale-similarity model,[1,2] the second variant of the ADM was shown to suffer from insufficient dissipation without secondary regularization (artificial viscosity). Stabilization was accomplished in the original ADM by adding a dissipative term to the right-hand sides of the momentum equations, namely

$$\chi(\bar{v}_j - \bar{u}_j), \tag{4}$$

where χ is an arbitrary damping parameter. Thus, in the ADM, deconvolution serves two distinct purposes: (i) modeling of residual stress [Eqs. (1) and (2)], and (ii) generation of high-order artificial dissipation [Eq. (4)].

Relative to conventional spatial filtering, time-domain filtering for LES offers certain conceptual and practical advantages[4–6] that have not previously received full consideration. Among these, (i) temporal LES (TLES) affords a natural bridge between direct numerical simulation (DNS) and Reynolds-averaged Navier-Stokes (RANS) methodologies, and (ii) temporal filters naturally commute with differentiation operators, making TLES attractive when commutation error is problematic, as is the case for LES on unstructured or highly stretched grids. The efficacy of TLES rests upon the premise that the removal of high-frequency content from the frequency spectrum should effectively remove high-wave-number content from the wave-number spectrum as well, so that TLES can be conducted at coarser temporal *and* spatial resolution than DNS. (See, for example, Fig. 5 of Pruett *et al.*[6]) In Pruett *et al.*,[6] the viability of TLES was established for viscous Burger's flow. In this paper, we develop a temporal variant of the ADM, the "TADM," describe modifications necessary to adapt approximate deconvolution from spatial to temporal filtering, and present results of the TADM for turbulent channel flow.

Although the residual-stress model of the TADM is *formally* identical to Eq. (1), adaptation to temporal filtering necessitates two modifications: (i) overlines now denote temporally rather than spatially filtered quantities, and (ii) the
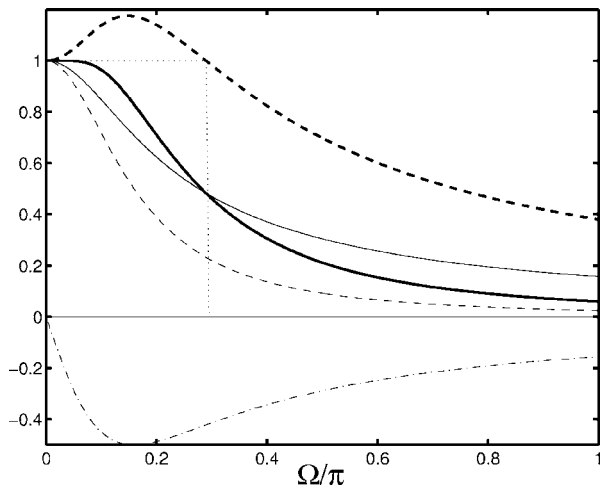
FIG. 1. Degree $p=3$ temporal deconvolution with optimized coefficients and $r=2$. Legend: H_r (dashed); H_i (dashed-dotted); $|H|$ (solid); $|\tilde{H}^{-1}|$ (heavy dashed); $|H*\tilde{H}^{-1}|$ (heavy solid); and spectral ideal (dotted).

values of coefficients C_k in Eq. (2) must be altered. By appending to the temporally filtered Navier-Stokes (NS) equations[6] [with dissipation term Eq. (4)] a set of auxiliary equations for the evolution of filtered fields, we obtain the closed system

$$\frac{\partial \bar{u}_j}{\partial x_j} = 0,$$

$$\frac{\partial \bar{u}_i}{\partial t} + \frac{\partial (\bar{u}_i \bar{u}_j)}{\partial x_j} = -\frac{\partial \bar{p}}{\partial x_i} + \frac{1}{Re}\frac{\partial^2 \bar{u}_i}{\partial x_j \partial x_j} - \frac{\partial M_{ij}}{\partial x_j} + \chi(\bar{v}_j - \bar{u}_j),$$

$$M_{ij} = \overline{v_i v_j} - \bar{v}_i \bar{v}_j,$$

$$v_i = \sum_{k=0}^{p} C_k \bar{u}_i^{(k+1)},$$

$$\frac{\partial}{\partial t}\bar{u}_i^{(k+1)} = \frac{\bar{u}_i^k - \bar{u}_i^{(k+1)}}{\Delta} \quad (1 \leq k \leq p),$$

$$\frac{\partial \bar{v}_i}{\partial t} = \frac{v_i - \bar{v}_i}{\Delta},$$

$$\frac{\partial}{\partial t}(\overline{v_i v_j}) = \frac{v_i v_j - \overline{v_i v_j}}{\Delta}. \tag{5}$$

The auxiliary equations of Eq. (5) arise from explicit time-domain filtering via a causal exponential filter in differential form, as discussed in Pruett et al.[6] The filter's transfer function is presented in Fig. 1. The nonvanishing imaginary part of the transfer function implies that causal filters, in general, introduce phase error in addition to amplitude modulation. For this reason, only the second variant (Eq. 9) of the ADM model of Stolz et al.[2] is viable in this context; for the first variant, the two terms of the model are relatively out-of-phase.

The differential form of the filter is advantageous for several reasons. First, the governing system is explicitly pa-

rametrized by the temporal filter width Δ. Second, the entire system, including the model, can be advanced forward in time consistently by the same numerical integration scheme. Finally, it is shown in Pruett et al.[6] that the parametrized system tends toward the NS equations in the limit of vanishing filter width, and (for stationary flows) toward the RANS equations in the limit of infinite Δ, provided the model is exact. For finite p, the TADM is inexact, which places practical limitations on Δ (or, in the discrete case, on the filter-width ratio $r \equiv \Delta/\Delta t$).

To implement the TADM, one must determine an appropriate order p, filter-width ratio r, and coefficients C_k. For the ADM, a single set of coefficients suffices both for residual-stress modeling and for secondary regularization. Because of the phase error[6] associated with causal filters, however, two distinct sets of coefficients are prescribed for the TADM: one set (C_k) optimized for the residual-stress model [Eq. (1)], the other (D_k) for secondary regularization, whereby in physical space the regularization operator becomes

$$\chi(\bar{w}_j - \bar{u}_j); \quad w_j = \sum_{k=0}^{q} D_k \bar{u}_j^{(k+1)}. \tag{6}$$

In Fourier space, the approximate deconvolution operator is $\tilde{H}^{-1} = \Sigma_{k=0}^{p} C_k H^k$, in which case the Fourier coefficients of v_j and u_j are related by $\hat{v}_j = H*\tilde{H}^{-1}\hat{u}_j$. For effective application to LES, the modulus of $|H*\tilde{H}^{-1}|$ should be shaped like a spectral (sharp cutoff) low-pass filter, so that low-frequency content is recovered faithfully while high-frequency content is attenuated. The binomial coefficients proposed for the ADM are unsuitable for the TADM. For the TADM, the coefficients C_k must be expressly designed to give $|H*\tilde{H}^{-1}|$ "near-ideal" properties.

To this end, we consider degree-3 deconvolution (i.e., $p=3$). The parameter space consists initially of four free parameters: $[C_0, C_1, C_2, C_3]$. The normalization constraint (no attenuation of the mean), which requires the coefficients to sum to unity, reduces the parameter space by one. Without loss of generality, $C_3 = 1 - C_0 - C_1 - C_2$. A further consideration involves the coefficient C_0. Unlike spatial filters, the transfer functions of causal filters do not vanish identically at the Nyquist frequency. Rather, they tend toward zero asymptotically. Consequently, as the frequency $\Omega \rightarrow \infty$, the deconvolution operator $H*\tilde{H}^{-1}$ decays slowly, as $1/\Omega$ if $C_0 \neq 0$, and as $1/\Omega^2$ if $C_0 = 0$. Because faster attenuation of high frequencies is highly desirable, C_0 is set to zero, implying that the deconvolved velocity is reconstructed only from fields that have been low-pass filtered at least twice.

The remaining parameters, C_1 and C_2, are determined by forcing the second and fourth derivatives of $|H*\tilde{H}^{-1}|$ to zero at $\Omega=0$ yielding algebraic equations. (Odd-ordered derivatives are identically zero at $\Omega=0$.) In general, the resulting equations are nonlinear and admit multiple solutions. Conjugate-symmetric complex solutions are discarded because they cannot be easily implemented in physical space. The remaining real solutions yield approximate inverses $\tilde{H}^{-1}$ that share the same moduli while differing in phase. In particular, for $p=3$, the method yields two real and two complex
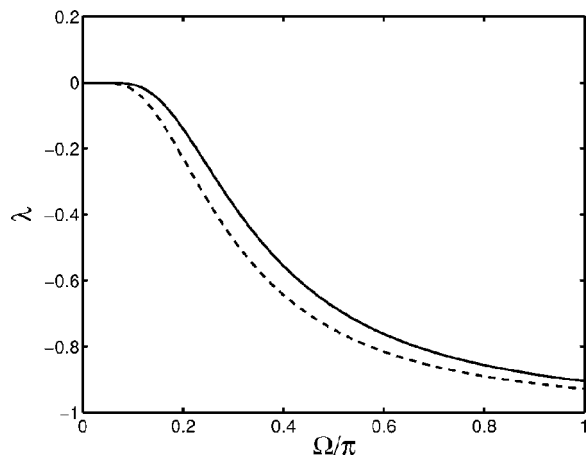
FIG. 2. Exponential decay rate $\lambda(\Omega)$ for temporal secondary regularization operators with optimized coefficients D_k, for $r=2$ and $\chi=1.0$. Legend: $q=3$ (solid); $q=2$ (dashed).

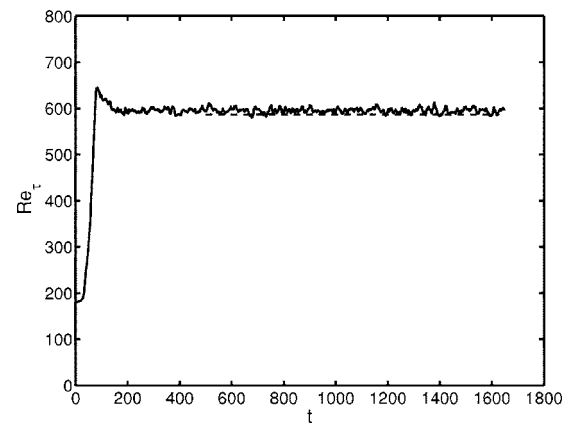FIG. 3. Evolution of instantaneous Re_τ (solid) relative to mean DNS reference value (dashed) for case TADM590.

solutions; the optimal real coefficients are $[0.0, \sqrt{6}, \sqrt{4+2\sqrt{6}}-2\sqrt{6}, 1-\sqrt{4+2\sqrt{6}}+2\sqrt{6}]$. Figure 1 presents the moduli of H, $\tilde{H}^{-1}$, and $H*\tilde{H}^{-1}$ for this coefficient set. Clearly the method can be extended to higher-degree deconvolution. To date, deconvolution degrees of 2, 3, 4, and 5 have been examined, as have a variety of deconvolution coefficient sets and filter widths. In all cases, the instantaneous and mean residual stresses are well defined, with means that have qualitatively correct profiles. In sum, temporal deconvolution appears to admit a robust family of residual-stress models.

A model problem for secondary regularization can be posed by considering $\hat{u}(t)=e^{i\omega t}$, which satisfies the differential equation of a harmonic oscillator, $d\hat{u}/dt=i\omega\hat{u}$. Secondary regularization functions as a dissipative term for the harmonic oscillator. With dissipation, the model problem becomes

$$\frac{d\hat{u}}{dt} = i\omega\hat{u} + \chi(\hat{w}-\hat{u}) = [i\omega + \chi(H*\tilde{H}^{-1}-1)]\hat{u}. \quad (7)$$

The dissipative term, the Fourier-space analog of Eq. (6), imposes exponential damping provided $Re[i\omega + \chi(H*\tilde{H}^{-1}-1)]<0.0$, which is satisfied if and only if

$$\lambda(\Omega) \equiv \chi\,Re(H*\tilde{H}^{-1}-1) < 0.0, \quad (8)$$

where the damping parameter $\chi>0$ scales the exponential decay rate $\lambda(\Omega)$. Inequality (8) is violated whenever the binomial coefficients are used for secondary regularization of

the TADM, leading to exponential growth in time at some frequencies.

For a given degree q, optimal coefficients can be found by setting derivatives of $Re[H*\tilde{H}^{-1}]$ to zero at $\Omega=0$. For $q=3$, there are three free parameters after normalization. Optimal coefficients are found by forcing the second, fourth, and sixth derivatives of $Re[H*\tilde{H}^{-1}]$ to zero, $\Omega=0$. (Again, odd-order derivatives vanish.) Specifically, the optimal coefficients for degree-3 temporal secondary regularization are $[D_0,D_1,D_2,D_3]=[35/16,-29/16,3/4,-1/8]$. The decay rate λ for this coefficient set is shown in Fig. 2 for $\chi=1$. Similarly, an optimal set of coefficients for degree-2 ($q=2$) secondary regularization is $[D_0,D_1,D_2]=[15/8,-9/8,1/4]$. Figure 2 also presents λ for $q=2$.

We have referred to p and q as defining the *degree* of the primary and secondary deconvolutions, respectively. It can be shown that the *orders* of the respective operators (as defined conventionally, the index of the first nonvanishing derivative with respect to Ω at $\Omega=0$ in Fourier space) are $2p$ and $2(q+1)$. The coefficient of 2 arises because the exponential filter is itself of second order.

The TADM was implemented for a simulation of plane channel flow at the nominal value of $Re_\tau=590$. A high-

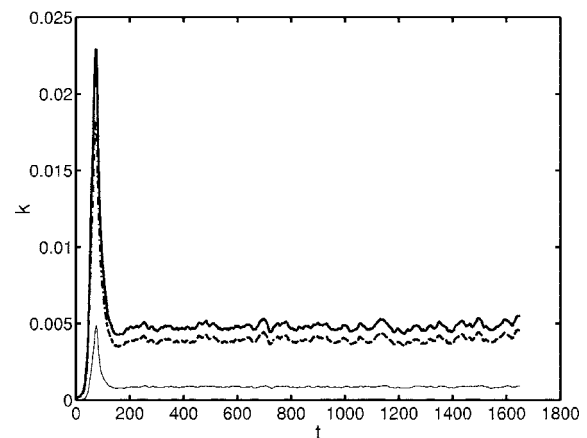TABLE I. Summary of test and reference cases at nominal $Re_\tau=590$.

Case	$N_x \times N_y \times N_z$	Δt	Re_τ	Model	(r,χ)
MKM590	$384\times384\times257$	—	587	none	NA
SAK590a	$48\times64\times65$	—	633	none	NA
SAK590b	$48\times64\times65$	—	574	ADM	NA
TADM590	$48\times64\times65$	0.04	595	TADM	(8,1.0)

FIG. 4. Turbulent kinetic energy for case TADM590. Legend: instantaneous $k[=\bar{k}+k_R]$ (heavy solid); $\bar{k}[=0.5\bar{\tau}_{ii}]$ (heavy dashed); $k_R[=0.5M_{ii}]$ (light solid).
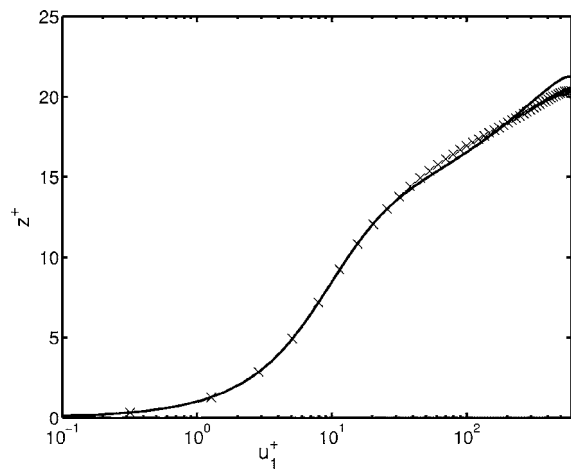
FIG. 5. Mean streamwise velocity vs z in wall units for case TADM590. Legend: DNS (solid); TADM (symbols, at grid points). Note that plot resolution is 1.5 times that of nominal wall-normal resolution (65 grid points) because physical-space data are extracted during dealiasing by 3/2 rule. At nominal resolution, first off-wall grid point lies at $z^+=u_1^+=0.717$.

quality statistical database (Moser *et al.*[7]) for DNS of this flow exists for purposes of validation. Moreover, channel flow has been investigated by Stolz *et al.*,[2] who used LES methodology with the ADM. Henceforth the DNS and ADM reference results will be referred to by the initials of their investigators, MKM and SAK, respectively. The DNS, LES, and TADM simulations each employ efficient pseudospectral numerical methods in space; the latter two exploit the code of Sandham and Kleiser.[8] For the TADM results presented, the flow was initialized to a randomly perturbed laminar state, allowed to transition, and then permitted to settle into a stationary state prior to the acquisition of statistics.

Table I and Figs. 3–6 summarize results of the TADM, with $p=3$ for both deconvolutions and no attempt to finely tune the model parameters. Three reference values of Re_τ are provided in the table: the target value of 587 from well-resolved DNS,[7] and no-model and ADM values obtained by
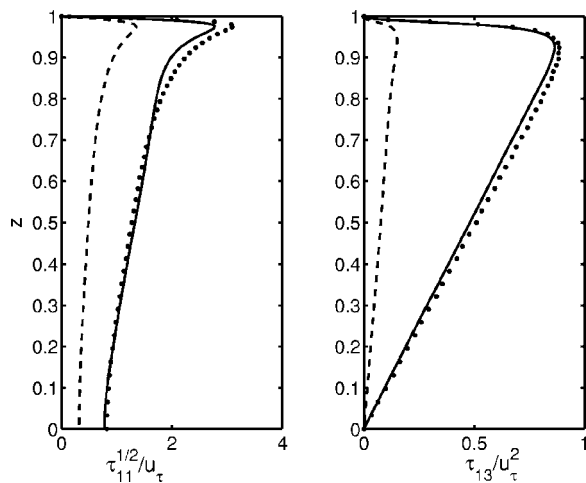
Stolz *et al.*,[2] who exploit the first variant of the ADM and dynamically determine the relaxation parameter χ. We note that all simulations were conducted at $Re_{bulk}=10935$, and that the computational workload of the coarse-grid ADM and TADM computations is some 400 times less than that of the reference DNS.

Figures 3 and 4 present the time evolution of instantaneous Re_τ and turbulent kinetic energy k, respectively, for the TADM. Note that the TADM is sufficiently robust to survive the strong peak in k during transition and that the model $k_R[\equiv 0.5M_{ii}]$ responds appropriately. The computed mean Re_τ for the TADM is just over 1% in error relative to the reference value of 587. Further, Fig. 5 shows reasonably good agreement of the mean streamwise velocity with DNS results. Finally, Fig. 6 presents selected components of Reynolds stress relative to their DNS counterparts, where the sum $\bar{\tau}_{ij}+\langle M_{ij}\rangle$ directly approximates the exact Reynolds stress τ_{ij} (without the need to filter the DNS results), and $\bar{\tau}_{ij}$ is the resolved-scale Reynolds stress. Note that the secondary (relaxation) term is not incorporated into the Reynolds-stress or k evaluation.

Finally, it might seem that the computational overhead for the TADM is high. However, storage issues are considerably ameliorated by the use of the differential form of the filter, and operation counts benefit both from the linearity of the auxiliary filter equations and the significant grid coarsening that TADM affords relative to fully resolved DNS.

In summary, TADM methodology admits a robust family of residual-stress models and deserves further consideration, particularly as an alternative to conventional (spatial) LES for applications in which spatial filtering is problematic, such as configuration LES.

FIG. 6. Reynolds stress for case TADM590. Legend: DNS (solid); TADM (symbols); $\langle M_{ij}\rangle$ (dashed).

[1]S. Stolz and N. A. Adams, "An approximate deconvolution procedure for large-eddy simulation," Phys. Fluids **11**, 1699 (1999).
[2]S. Stolz, N. A. Adams, and L. Kleiser, "An approximate deconvolution model for large-eddy simulations with application to incompressible wall-bounded flows," Phys. Fluids **13**, 997 (2001).
[3]S. Stolz, N. A. Adams, and L. Kleiser, "The approximate deconvolution model for large-eddy simulations of compressible flows and its application to shock-turbulent-boundary-layer interaction," Phys. Fluids **13**, 2985 (2001).
[4]Y. M. Dakhoul and K. W. Bedford, "Improved averaging method for turbulent flow simulation. Part I: Theoretical development and application to Burgers' transport equation," Int. J. Numer. Methods Fluids **6**, 49 (1986).
[5]C. D. Pruett, "On Eulerian time-domain filtering for spatial large-eddy simulation," AIAA J. **38**, 1634 (2000).
[6]C. D. Pruett, T. B. Gatski, C. E. Grosch, and W. D. Thacker, "The temporally filtered Navier-Stokes equations: Properties of the residual stress," Phys. Fluids **15**, 2127 (2003).
[7]R. D. Moser, J. Kim, and N. N. Mansour, "Direct numerical simulation of turbulent channel flow up to Re_τ=590," Phys. Fluids **11**, 943 (1999).
[8]N. D. Sandham and L. Kleiser, "The late stages of transition to turbulence in channel flow," J. Fluid Mech. **245**, 319 (1992).